CHARACTERIZATION OF MEDIUM VOLTAGE EQUIPMENT AGEING BY MONITORING OF PARTIAL DISCHARGES CHEMICAL AND ACOUSTICAL EMISSION

Emmanuel Odic, Jouseau Eric, Vivien Gaëtan, Maroni Claire-Sophie

CHARACTERIZATION OF MEDIUM VOLTAGE EQUIPMENT AGEING BY MONITORING OF PARTIAL DISCHARGES CHEMICAL AND ACOUSTICAL EMISSION

E. Odic*, E. Jouseau**, G. Vivien**, C-S. Maroni**

*Département Energie, Supélec, Gif-sur-Yvette, FRANCE **Schneider Electric SA, Grenoble, FRANCE

INTRODUCTION

During the ageing of in-service medium voltage equipment, electrical losses are mainly due to partial discharges. These partial discharges can lead to the electrical failure of industrial equipment [1]. Partial discharges include (i) bulk discharges occurring in insulating material voids, (ii) corona discharges affecting or not the insulator and (iii) surface discharges developing on an insulator surface from a triple point (conductor/insulating material/air). Bulk and surface discharges can respectively lead to a final volume or surface breakdown whereas corona discharges may only induce a long term chemical surface ageing.

Non-intrusive diagnostic methods are then required for predictive qualitative analysis that can warn of a potential upcoming system failure of medium voltage electrical equipment. Within these methods, electrical partial discharge analysis [2,3] (fast transient current signal associated the discharge phenomena measured at the medium voltage side using capacitors or Rogowski coil sensors) is currently applied to detect any damage or insulation failure which may have occurred during shipment and installation. Although this electrical method provides accurate recordings of partial discharges in laboratory conditions, it is difficult to implement for in-service equipment, such as power transformers, because of the high level of electromagnetic interference [3]. Two alternative non-intrusive methods have been investigated in this study: acoustical detection and gas phase chemical detection. Acoustic emission detection techniques have been applied to transformer partial discharge detection since the 1950s (liquid medium transformers) [2]. Electrical and acoustical procedures are often employed jointly, the acoustic technique being more effective for the location of the discharge sites [2]. In the present study, ultrasonic acoustic emission was directly investigated on medium voltage equipment subjected to accelerated ageing; collected experimental data were correlated to simultaneous electrical partial discharge analyser recordings.

Gas phase detection of chemical species produced and released in atmospheric air is limited to the specific cases of surface discharges and corona discharges. These gaseous products can be identified and their formation rate evaluated by a periodic sampling of the ambient air in the vicinity of the discharge zone. For this method, preliminary laboratory-scale investigations were first realized.

In view to implement both of the two methods on in-service equipment, chemical and acoustic measurements were simultaneously performed on a power transformer.

FUNDAMENTALS

Focussing on corona discharge and surface discharge, i.e. electrical gas discharges occurring in ambient atmosphere, ionisation phenomena are initiated in the high electrical field region respectively resulting from the conductor geometry (wire, point, sharp edge) or from a triple point (metallic conductor / insulation material / gas). According to the conductor geometry, applied voltage amplitude and polarity, ionisation phenomena will be confined in the vicinity of the high field region or will propagate in gas from this region as transient successive ionisation waves (streamer regime with current pulses associated with the development of filamentary discharges). In any case, electron inelastic collisions will also lead to gas molecules dissociation and excitation resulting in chemical active species formation and light emission; elastic collision between ions and neutral molecules will result in local gas heating. Light, gaseous chemical reactants and heating are consequently evidence of gas discharges.

Acoustic Phenomena

The acoustic emission of atmospheric pressure arc discharges was previously studied [5]. It was stated that within the three different mechanisms potentially able to induce the creation of acoustic waves (i.e. momentum transfer, energy transfer and mass transfer), energy transfer is predominating, namely through thermal transfer in the case of atmospheric pressure arc discharges. The acoustic wave magnitude A_a can then be correlated to the energy H transferred to the discharge:

$$A_a = K \times \frac{M}{k_B T_g} \times \frac{\partial H}{\partial t} \qquad (1)$$

where M is the mass of gas in which the arc is burning, T_g the initial temperature of this mass of gas, k_B the Boltzmann's constant and K a constant proportionality coefficient. In equation (1), the $\partial H / \partial t$ term can replaced by $\gamma \times \partial P / \partial t$ where P is the arc input power and γ the heat capacity ratio $C_p / C_v = 7/5$ for diatomic gases:

$$A_a = K \times \frac{M}{k_B T_g} \times \gamma \frac{\partial P}{\partial t} \qquad (2)$$

This relationship was experimentally confirmed by [5] in the case of arcs burning at atmospheric pressure.

Later on, similar experiments were carried out in a thermodynamic non-equilibrium system, i.e. with an ac point-to-plane dielectric discharge burning in air at atmospheric pressure in a streamer regime [6]. Under these conditions, all filamentary discharges propagate with negligible voltage drops and for very similar onset voltage values. The discharge current I then replaced, with a K' proportionality factor, the discharge input power term of (2):

$$A_a = K' \times \frac{M}{k_B T_g} \times \gamma \frac{\partial I}{\partial t} \qquad (3)$$

Equation (3) was simplified, using I_{max}, the amplitude of the current pulses associated to the propagation of filamentary discharges (streamers), instead of $\partial I / \partial t$. This approximation was supported by an experimental linear correlation found between A_a and I_{max}. Plasma temperature values obtained by spectroscopic measurements in the vicinity of the point electrode during the emissive phase (streamer propagation) ranged from 420 K to 480 K with increasing values of I. It was then stated that the overpressure wave corresponding to the acoustic wave can be attributed to a local transient temperature variation: the transient heating of the gas gap volume by the discharge (50-100 ns) is followed by different cooling mechanisms, i.e. slow phenomena (conduction, diffusion) enhanced by the electrical wind effects, and rapid phenomena such as an adiabatic expansion [7]. If the relaxation time between two successive streamer events is long enough ($\approx$ 100 - 300 µs) the gas can be cooled down to room temperature.

Gas Chemistry

Besides of overpressure waves (acoustic waves) initiation, local gas temperature obviously influences the chemical properties of corona and surface discharges (list of reactions presented in Table 1). The temperature here under consideration is the mean temperature (not instantaneous temperature value) in the gaseous reactive volume.

In gas mixtures containing oxygen such as air, the major discharge product is ozone. For its formation, the first step is molecular oxygen dissociation by direct electron impact (reaction (4) in Table 1). A three body recombination reaction of the released oxygen radical leads to the formation of ozone (5). This mechanism is balanced by a partial destruction of the formed ozone (6). It is worthy of note that ozone formation kinetics is lowered when gas temperature increases because its destruction is promoted over its formation.

In air, nitrogen oxides N_2O, N_2O_5, NO, NO_2 (and associated acids HNO_2, HNO_3 in presence of water vapour) are also produced. N_2O and NO are formed at low temperature (reactions (7) and (8) of Table 1), i.e. in presence of ozone; NO is in turn oxidized into NO_2 (9). N_2O_5 comes from the oxidation of NO_2 into NO_3 (10), unstable intermediate, reacting with another NO_2 molecule (11).

With temperature, nitrogen oxides formation is increased and ozone net production can decrease to zero. Under these conditions, N_2O_5 is not produced and NO is emitted since it is no longer oxidized by ozone. Ozone appears then as a low temperature product. NO_2 is associated to medium temperature discharge conditions. NO is the evidence of high temperature conditions. This was supported by experimental results [15] showing that, in identical operating conditions, the nature of these stable gaseous products and their relative distribution of concentration (measured by means of FTIR absorption spectroscopy) were closely correlated to the discharge instantaneous temperature (see Figure 1). Note that this temperature T_{pl} is not the mean temperature to be injected in the reaction kinetics constants of Table 1, but is rather a characteristic of the discharge regime; nevertheless, T_{pl} influences the mean temperature of the gaseous volume in which chemical reactions take place.

As the discharge regime approaches breakdown (spark discharge), the T_{pl} value and thus the mean gas temperature increases. The discharge regime can so be identified thanks to the analysis of the gaseous products emitted in the ambient atmosphere.

TABLE 1 Major reactions of gas discharges burning in oxygen / nitrogen mixtures

| reaction	kinetics constants	Ref.	#
$e + O_2 \rightarrow e + O + O$	$\sigma_{max} = 2.25 \times 10^{-18}$ cm^2	[8]	(4)
$O + O_2 + M \rightarrow O_3 + M$	$k_1 = 5.58 \times 10^{-29}.T^{-2}$ cm^{6}s^{-1}molec^{-2} for M = N_2 $k_2 = 8.6 \times 10^{-31}.T^{-1.25}$ cm^{6}s^{-1}molec^{-2} for M = O_2	[9] [10]	(5)
$O_3 + M \rightarrow O + O_2 + M$	$k_3 = 73 \times 10^{-11}$ exp(-11400/T) cm^{3}s^{-1}molec^{-1} for M = O_2 $k_4 = 2.1 \times 10^{-5}$ T$^{-1.5}$exp(-12300/T) cm^{3}s^{-1}molec^{-1} for M = N_2	[11] [12]	(6)
$N_2 + O_2 \rightarrow N_2O + O$	$k_5 = 11 \times 10^{-11}$ exp(-23400/T) cm^{3}s^{-1}molec^{-1}	[11]	(7)
$N_2 + O_2 \rightarrow 2$ NO	$k_6 = 3.1 \times 10^{-11}$ cm^{3}s^{-1}molec^{-1}	[13]	(8)
$NO + O_3 \rightarrow NO_2 + O_2$	$k_8 = 3.6 \times 10^{-12}$ exp(-1560/T) cm^{3}s^{-1}molec^{-1}	[11]	(9)
$NO_2 + O_3 \rightarrow NO_3 + O_2$	$k_c = 1.2 \times 10^{-13}$ exp(-2450/T) cm^{3}s^{-1}molec^{-1}	[13]	(10)
$NO_3 + NO_2 + M \rightarrow N_2O_5 + M$	$k_{10} = 5.3 \times 10^{-20}.T^{-4.1}$ cm^{6}s^{-1}molec^{-2} for M = N_2	[14]	(11)
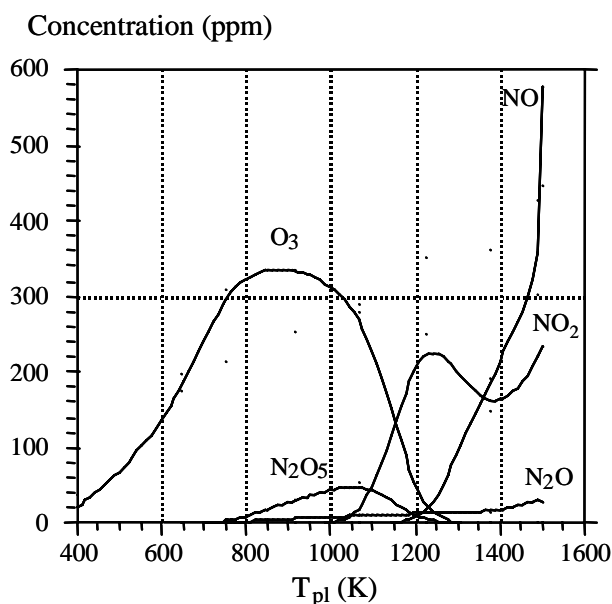
Concentration (ppm)

Figure 1 Concentration of discharge stable gaseous products as a function of the plasma temperature T_{pl}. Point-to-plane dielectric barrier discharge. Feed gas: dry air.

LABORATORY SCALE EXPERIMENTS

The aim of the laboratory scale study was (i) to test low cost chemical sensors for the detection of ozone and nitrogen oxides and (ii) to identify a pre-breakdown discharge regime for a single discharge even though numerous discharges were running in a conventional non-disruptive regime.

Discharge Set-Up

Experiments were carried out in an open chamber (27 l, ambient atmosphere) containing a single discharge system consisting of a point-to-plane metallic electrodes arrangement (Figure 2).
The point electrode is connected to a 45 kHz high voltage power supply (0-20 kV peak). The plane electrode, connected to ground, is covered with a dielectric ceramic disc (Al_2O_3 / SiO_2, 60 mm diameter, 3 mm thickness). The air gap between the point tip and the dielectric surface is fixed to 2.5 mm.
The dielectric plate is bored 5 mm from the point-to-plan axis, so that when the applied voltage increases up to a critical voltage V_{cr}, the discharge expands on the insulator surface until reaching the default and so simulates the situation of a defective insulation. In this case, a spark discharge regime is obtained. Below the V_{cr} voltage value, the discharge is running in a regular dielectric barrier discharge regime, so simulating a healthy insulator. Discharge current and applied voltage are recorded but not discussed in this paper.
An ozonizer fed with dry air is used to inject ozone (40 ppm in dry air at 170 l/h) in the experimental chamber, so simulating numerous gas discharges burning in a steady state regime.

Gas detection device

The chamber atmosphere is sampled with a 130 l/h fixed flow rate. Ozone concentration in the sampled gas is measured using UV absorption spectroscopy (254 nm). For gas detection, a SnO_2 semi-conductor gas sensor is used. When a SnO_2 crystal is heated in air, oxygen is adsorbed on its surface, so attracting the donor electrons from the crystal and then forming a surface potential. This surface potential serves as a potential barrier against electron flow. The electrical resistance Rs of the sensor is attributed to this potential barrier. In the presence of an oxidizing gas, Rs increases. In the presence of a deoxidizing gas, Rs decreases. An ozone destruction device is used to specifically detect nitrogen oxides since the metal oxide sensor used has a high sensitivity (0.1 ppm NO_2) but a poor selectivity of NO_2 vs. O_3. The ozone destruction device consists of an oven (150°C) filled with an Al_2O_3 molecular sieve. As depicted in Figure 2, two gas sensors are used, one placed upstream of the oven (Rs1 signal), the other one downstream of the oven (Rs2 signal).

Results

Obtained results are presented in Figure 3 where Rs1 and Rs2 values are plotted as a function of time. The measured concentration of ozone in the sampled gas is also reported in the same figure. At $t = 0$, a regular dielectric barrier discharge (DBD) is ignited. Both Rs1 and Rs2 values increase and reach a maximum value at $t = 2.5\,min$ corresponding to a 7.2 ppm ozone concentration. The rise of Rs1 corresponds to the rise of ozone concentration. The rise of Rs2 corresponds to the formation of NO_2. Ozone and NO_2 are produced by the discharge. At $t = 5\,min$, ozone produced by the external ozonizer is introduced into the chamber. A 26.4 ppm maximum ozone concentration is reached. Since the ozonizer is fed with air, NO_2 is also formed.
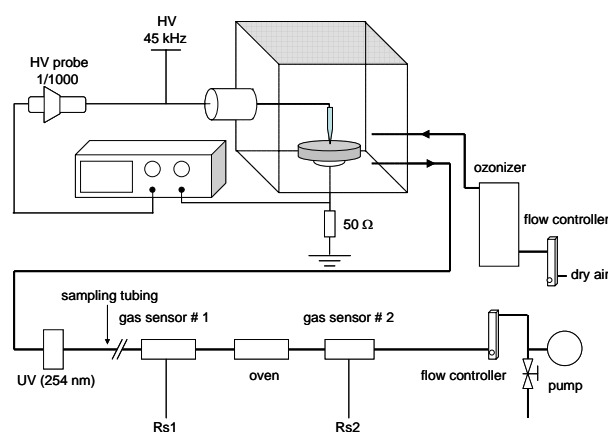

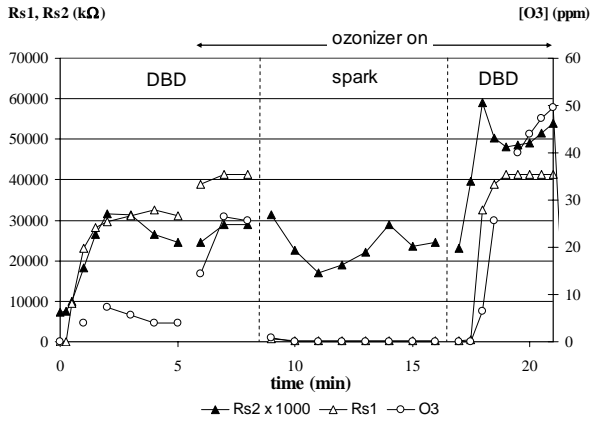Figure 2 Block diagram of the complete experimental set-up.

Figure 3 Rs1 /Rs2 values and ozone concentration in the sampled gas vs. time.

The values obtained for Rs1 and Rs2 so proportionally increase with respect to the specific response for each gas species. At $t = 8.5\,min$, the applied voltage is raised to its V_{cr} critical value and a spark discharge regime is obtained. Under these conditions, NO is the major product formed by the discharge. The ozone concentration drops to a value inferior to its detection limit. This means that (i) O_3 is no more produced by the discharge and (ii) the introduced O_3 is reacting with NO to form NO_2 (reaction (9) in Table 1). The Rs1 signal decrease is then due to the ozone concentration drop. The Rs2 signal decrease is due to the NO formation (NO is a deoxidizing species compared to NO_2). The slight increase of Rs2 at $t = 11\,min$ is due to the NO_2 formation. Not visible on this due to vertical scale, Rs1 is also slightly increasing.

At $t = 16.5\,min$, the applied voltage is lowered in order to come back to a DBD regime. NO is then no longer formed by the discharge. Ozone produced by the discharge and introduced by the ozonizer external device react with the NO accumulated in the chamber to produce large amounts of NO_2. Rs2 is then rising to a level exceeding its previous DBD regime value. The Rs1 response is delayed because ozone is mainly consumed by the NO oxidation (as confirmed by the UV ozone measurement) during this transition phase.

Note that when both the ozonizer and the studied discharge are turned off, the Rs1 and Rs2 values reach their initial values within 3 minutes. A comparable figure is obtained, with the same evolution for Rs1 and Rs2 values, when the DBD discharge regime is simulated by NO_2 (standard 100 ppm NO_2 in N_2) introduction and the spark discharge regime by NO (standard 90 ppm NO in N_2) introduction.

These laboratory scale experiments show that, using the gas sampling device with low cost metal oxide gas sensors, the DBD to spark regime transition of a single discharge can be detected in an ozone emitting environment (i.e. numerous discharges simultaneously running in a regular DBD regime).

MEDIUM VOLTAGE EQUIPMENT AGEING EXPERIMENTS

The same gas detection device is tested on a dry transformer (630 kVA, 400 V/20 kV) submitted to a Highly Accelerated Life Testing (HALT). As moisture is a major factor for surface discharge activity, it is used to study the transient acoustical and chemical emission of these discharges when the voltage applied to the transformer is switched from 0 to its nominal value *Un* (400 V) under extreme wet conditions (100 % Relative Humidity at 17°C).
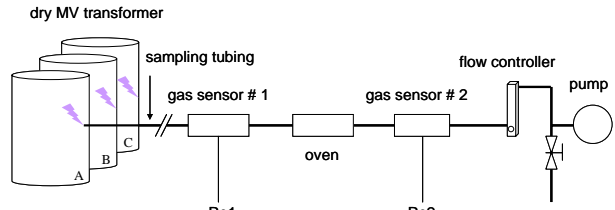

Figure 4 Schematic block diagram of the medium voltage power transformer experiment.
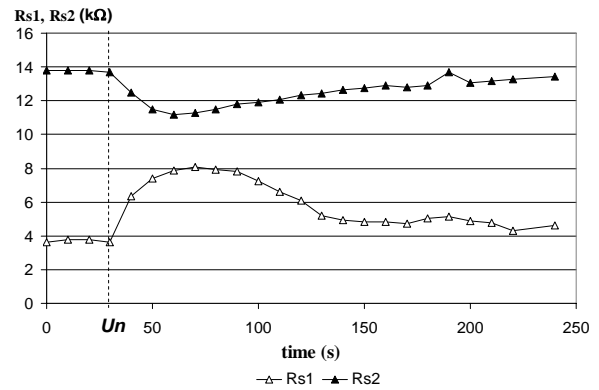

Figure 5 Rs1 /Rs2 values vs. time. Direct switch to Un (at $t = 30\,s$) under 100 % RH moisture conditions.
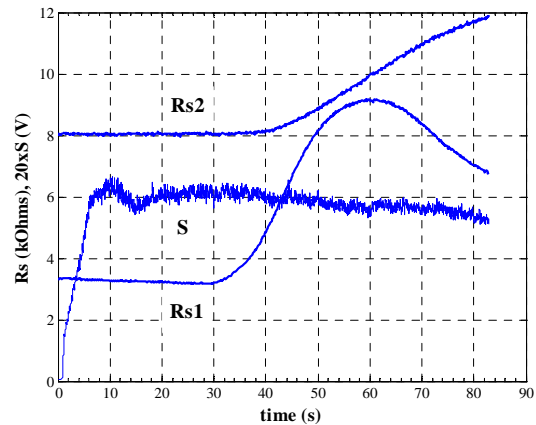

Figure 6 Rs1 /Rs2 values and rms acoustic signal S vs. time. Direct switch to Un (at $t = 0\,s$) under 100 % RH moisture conditions.

Figure 5 exhibits results obtained by sampling (130 l/h) the atmosphere in the vicinity of the coupling bar connector of the A phase winding (see Figure 4). 10 seconds after switching on the voltage, gas sensors detect a discharge activity. Looking at the Rs1 signal, a rise is observed, corresponding to ozone and NO_2 emission. Simultaneously, Rs2 decreases, so detecting the emission of NO. Gas discharge phenomena tend to dry the insulator surface on which they propagate; their activity is then progressively reduced. Rs2 tends to reach its initial value whereas Rs1 decreases and stabilizes at a value slightly higher than its initial value, so evidencing a regular DBD regime discharge activity. Gas chemical measurement so allowed to (i) detect a surface / gas discharge activity within a few seconds after ignition (ii) detect a reversible transition through spark discharge regime (NO emission).

An acoustical detection can be jointly realized. The ultrasonic sensor (20 kHz – 800 kHz frequency range) is an accelerometer mounted externally on the equipment enclosure. This sensor actually measures the transformer enclosure vibration induced by the discharges acoustical emission. The signal is acquired with a 2 MHz sampling rate. Specific measurements obtained with this sensor during Highly Accelerated Life Testing (HALT) of the transformer have been previously published [16]. Figure 6 presents results of joint acoustical and gas chemical measurement obtained in the same operating conditions as those presented in Figure 5 except that several tests have been carried out in between. The insulator surface has then been dried by the successive discharge events. Consequently, if a transient rise of the discharge activity shown by the maximum value reached by Rs1 (corresponding to a rise of the ozone production) is observed (see Figure 6), the transition to spark discharge regime is no longer observed since Rs2 is monotonously increasing (constant increase of NO_2 production). The rms value S of the acoustical signal also depicted in Figure 6 as a function of time, exhibits a shape similar to the Rs1 profile. S reaches a maximum value at $t = 10\,s$ (maximum discharge activity) when Rs1 maximum is 50 s delayed. Consistent results are so observed with the acoustical and chemical sensors, but with different time constants (while the acoustic system gives a near instantaneous response, the chemical system is delayed by a combination of delays caused by the gas sampling and the intrinsic metal oxide sensor response time).

CONCLUSION

Thermal properties of gas discharges lead: (i) through transient variations to acoustic emissions, (ii) through slower heat exchanges to increase the mean temperature of the local gas volume and so modify the gas chemistry. The acoustical method can provide fast and reliable information on partial discharge activity. Furthermore, this technique can allow detection of the location of the emitting discharge. Gas phase chemical detection is obviously limited to the detection of gas discharges (corona and surface discharges). But it is shown that using this technique, gas discharges can be detected within a few tens of seconds from their onset. Furthermore, gas sensing can be able to detect the spark discharge regime transitions (signifying risks of surface breakdown) of a single discharge location. An equipment enclosure ambient air sampling coupled with an acoustical technique can be used to estimate the discharge activity and to detect a discharge regime transition; such a combined measurement can then be an accurate method for determination of the state of health of medium voltage equipment.

REFERENCES

1. Golubev, A; Kane, C *On-line insulation condition assessment on power transformers.*

2. Bartnikas,R, Partial discharges : their mechanisms, detection and measurements, IEEE Trans. on dielectrics and electrical insulation, Vol. 9, n°5, pp. 763-808 (2002).

3. *Experience with online partial discharge analysis as a tool for predictive maintenance for medium-voltage switchgear systems* IEEE industry applications magazine September/October 2004.

4. Yu B, Kim DW, Deng J, Xiao H, Wang A Fiber Fabry-Perot *Sensors for detection of partial discharges in power transformers.*

5. Fitaire, M, *Bruits Acoustiques des Arcs Electriques*, in l'Arc Electrique et ses Applications, Club EDF-Arc Electrique – Tome 1, Ed. du CNRS (1984).

6. Odic E., Dhainaut M., Goldman A., Goldman M., Dessante Ph. *Study in space and time of the gas temperature variations in dielectric barrier discharge reactors* in J. Adv. Oxid. Technol., Vol. 8, N°2, Science & Technology Network, Inc., pp. 133-141 (2005).

7. Marode, E; Samson, S; Djermoune, D; Deschamps, N; Touzeau, M; De Souza, R, *Time resolved Temperature Measurements and Computation of Streamer Air Discharge and Diffusion Controlled Chemistry*, J. Adv. Oxid. Technol., **4**, 3 (1999).

8. Hollahan, J R; Bell, A T, *Techniques and applications of plasma chemistry*, Wiley InterScience, New York (1974)

9. Pignolet, P.; Hadj-Ziane, S.; Held, B.; Peyrous, R.; Benas, J. M.; Coste, C., *Ozone generation by point-to-plane corona discharge*, J. Phys. D : Appl. Phys., 23, 1069-1072 (1990).

10. Kossyi, I. A.; Kostinsky, A. Yu.; Matveiev, A. A.; Silakov, V. P.; Plasma Source Sci. Technol., 1, 207-220 (1992).

11. Baulch, D.L.; Drysdale, D.D.; Duxbury, J.; Grant, S. Eds, Evaluated Kinetic Data for High

Temperature Reactions, 3, Buttersworths, London, UK, (1976).

12. Eliasson, B.; Kogelschatz, U.; Baessler, P.; J. Phys. B : At. Mol. Phys., 17, L797-801 (1984).

13. Peyrous,R, *Simulation de l'évolution temporelle de diverses espèces gazeuses créées par l'impact d'une impulsion électronique dans de l'oxygène ou de l'air sec ou humide*, thèse d'état, Université de Pau et des Pays de l'Adour (1986)

14. Peyrous, R, *The effects of relative humidity on ozone production by corona discharge in oxygen or air – A numerical simulation – Part II*, Ozone Science Engineering, Vol. 12, pp. 41-64 (1990)

15. Odic, E.; Parissi, L.; Goldman, A.; Goldman, M.; Koch, S., *Chemical by-products in Air, with Admixtures in Correlation with the Gas Temperature Enhanced by Non Equilibrium Discharges*, in Proc. 2nd Intern. Symp. on Non thermal Plasma Technology for Pollution Control Proc., pp. 107-112 (1997).

16. Jouseau, E.; Maroni, C-S.; Odic, E.; Vivien, G.; *Exhibition of an ageing criterion based on partial discharge detection for medium voltage equipment* in Proc. 5th IEE Intern. Symp. on Diagnostics, Electrical Machines, Power Electronics and Drivers, pp. 301-305 (2005).